INTERNATIONAL JOURNAL FOR NUMERICAL METHODS IN FLUIDS, VOL. 11, 341–353 (1990)

# LOCALLY MASS-CONSERVING TAYLOR–HOOD ELEMENTS FOR TWO- AND THREE-DIMENSIONAL FLOW

R. W. THATCHER

*Department of Mathematics, UMIST, PO Box 88, Manchester M60 1QD, U.K.*

SUMMARY

By supplementing the pressure space for Taylor–Hood elements, elements that satisfy continuity locally are produced. These elements are shown to satisfy the Babuska–Brezzi compatibility condition by using the patch argument.

Two examples are presented, one illustrating the convergence rates and the other illustrating a difficulty with a Taylor–Hood element that is overcome by the element presented here.

KEY WORDS Finite element techniques Incompressible flow

## 1. INTRODUCTION

A popular triangular element for solving fluid flow problems was introduced by Hood and Taylor.[1] It is a quadratic velocity, linear pressure element providing continuous approximations to both velocity and pressure and is often referred to as the $P_2/P_1$ element for fluid flow. More recently the quadrilateral and hexahedral elements $Q_2/Q_1$ have also been referred to as Taylor–Hood elements. These are biquadratic (or triquadratic) velocity and bilinear (or trilinear) pressure on the standard element providing continuous approximations for velocity and pressure. Indeed, $P_k/P_{k-1}$ triangular and $Q_k/Q_{k-1}$ quadrilateral and hexahedral elements are all often referred to as Taylor–Hood elements for all $k \geq 2$. In this paper we shall only consider the case $k=2$, but the remarks apply for all $k \geq 2$; the analysis, however, becomes somewhat lengthy for $k > 2$.

It has been known for some time that one of the drawbacks in using continuous pressure elements is that continuity or mass conservation is only obtained over the whole region and not over individual elements. This has been noted in at least three papers,[2–4] each group of authors putting down the poor results to lack of mass conservation at the element level and then moving over to some form of discontinuous pressure solution to provide mass conservation within the element. The elements adopted each provided much improved solutions, although the improvement was not necessarily the result of element mass balance. Tidd *et al.*[4] supplemented the $P_2/P_1$ with piecewise constant pressures, the subject of the analysis here, which was an idea for triangular elements first suggested by Griffiths.[5] Gresho *et al.*[2] supplemented the $Q_2/Q_1$ element with piecewise constants, but although this gave a significant improvement, they preferred the $Q_2/P_1$ element (fully discontinuous linear pressures in a quadrilateral element).

The subject of this paper is the analysis of supplementing Taylor–Hood elements with piecewise constant pressures using the patch argument introduced by Boland and Nicolaides,[6] but

0271–2091/90/110341–13$06.50 *Received September 1989*

considerably extended and simplified by Stenberg[7] using the ideas of Verfürth[8] on mesh-dependent norms.

## 2. THE STOKES EQUATIONS AND THE MACROELEMENT TECHNIQUE

In this section we shall reproduce the notation and main theoretical results contained in Stenberg.[7] The weak form of the Stokes equations in a region $\Omega \subset R^d$, $d=2$ or 3, is to find $u \in H_0^1(\Omega)^d$ and $p \in L_0^2(\Omega)$ such that

$$\begin{aligned} \nu(\nabla u, \nabla v) - (\operatorname{div} v, p) &= (f, v), \\ (\operatorname{div} u, q) &= 0 \end{aligned} \tag{1}$$

for every $v \in H_0^1(\Omega)^d$ and $q \in L_0^2(\Omega)$, where $(,)$ and $L_0^2(\Omega)$, $H_0^1(\Omega)$ are the usual inner product and function spaces. The mixed finite element method is to choose finite element spaces $V_h$ and $P_h$ and find $u_h \in V_h \subset H_0^1(\Omega)$ and $p_h \in P_h \subset L_0^2(\Omega)$ such that

$$\begin{aligned} \nu(\nabla u_h, \nabla v) - (\operatorname{div} v, p_h) &= (f, v), \\ (\operatorname{div} u_h, q) &= 0 \end{aligned} \tag{2}$$

for every $v \in V_h$ and $q \in P_h$, where $h$ is the usual finite element parameter. The spaces $V_h$ and $P_h$ cannot be chosen arbitrarily, but if the Babuska–Brezzi condition

$$\inf_{\substack{p \in P_h \\ p \neq 0}} \left\{ \sup_{\substack{v \in V_h \\ v \neq 0}} \left\{ \frac{(\operatorname{div} v, p)}{\|v\|_1 \|p\|_0} \right\} \right\} \geq \beta > 0 \tag{3}$$

holds, then the following theorem is proved (see e.g. Reference 9).

*Theorem 1*

If $V_h$ and $P_h$ satisfy (3), then (2) has a unique solution $(u_h, P_h)$ satisfying

$$\|u - u_h\|_1 + \|p - p_h\|_0 \leq C \left\{ \inf_{v \in V_h} \|u - v\|_1 + \inf_{q \in P_h} \|p - q\|_0 \right\}, \tag{4}$$

where $(u, p)$ is the solution of (1). Moreover, if $\beta$ in (3) is independent of $h$, so is $C$ in (4).

The first breakthrough to simplify the proof of (3) for particular spaces $V_h$ and $P_h$ was given by Boland and Nicolaides.[6] Stenberg[10] independently found a similar result, but here we are using the modified theory of Stenberg.[7]

A finite element partitioning of $\bar{\Omega}$ is denoted by $C_h$, all the elements of which are assumed to be triangles or convex quadrilaterals in $R^2$, or tetrahedra or convex hexahedra in $R^3$. The partitioning is assumed to satisfy the usual regularity conditions[11] but is *not* assumed to be quasi-uniform. The reference element is denoted by $\hat{K}$ and the standard mapping from $\hat{K}$ to $K$ is denoted by $F_k$.

A macroelement $M$ is defined as a connected set of elements, and two macroelements $M$ and $\tilde{M}$ are said to be equivalent if they can be mapped continuously onto each other; see Reference 7 for more details of this. Over $C_h$ there is a velocity interpolation space $\tilde{V}_h$ and a pressure interpolation space $\tilde{P}_h$ with all velocity and pressure nodal values unconstrained and from which we obtain

$$\begin{aligned} V_h &= \tilde{V}_h \cap (H_0^1(\Omega)^d, \\ P_h &= \tilde{P}_h \cap L_0^2(\Omega). \end{aligned}$$

Over the macroelement $M$ we define two spaces $V_{0,M}$ and $P_M$ by:

(i) Let $\tilde{v} \in \tilde{V}_h$ with $\tilde{v}=0$ at every velocity node on $\delta M$ and outside $M$ and let $v$ be the restriction of $\tilde{v}$ to $M$; then

$$V_{0,M} = \{\text{set of all such } v\}.$$

(ii) Let $\tilde{p} \in P_h$ with all $\tilde{p}=0$ at every pressure node outside $M$ and let $p$ be the restriction of $\tilde{p}$ to $M$; then

$$P_M = \{\text{set of all such } p\}.$$

Further we denote

$$N_M = \{p \in P_M \text{ such that } (\operatorname{div} v, p)_M = 0 \text{ for every } v \in V_{0,M}\}. \tag{5}$$

Finally we denote by $\Gamma_h$ the collection of edges ($d=2$) or faces ($d=3$) of the elements of $C_h$ in the interior of $\Omega$. Stenberg[7] proved the following theorem.

*Theorem 2*

Suppose that there exists a fixed set of equivalence classes $E_i$, $i=1, 2, \ldots, q$, of macroelements, a positive integer $L$ and a macroelement partitioning $M_h$ such that:

(M1) For each $M \in E_i$ the space $N_M$ consists of functions that are constant on $M$ for $i=1, 2, \ldots, q$.
(M2) Each $M \in \mathrm{M}_h$ belongs to one of the classes $E_i$, $i=1, 2, \ldots, q$.
(M3) Each $K \in C_h$ is contained in at least one and not more than $L$ macroelements of $M_h$.
(M4) Each interior edge ($d=2$) or face ($d=3$) belonging to $\Gamma_h$ is contained in at least one and not more than $L$ macroelements of $M_h$.

Then the stability inequality (3) is valid. ($\beta$ will be independent of $h$ provided $q$ and $L$ are independent of $h$.)

We shall now apply this result to various Taylor–Hood elements in which the continuous pressure space has been supplemented by piecewise constants.

*Regular grids of rectangular elements*

In this subsection we shall assume that $C_h$ is a regular grid with grid lines parallel to the $x$- and $y$-axes. In this case

$$V_h = \{u \in (H^1(\Omega))^2 \mid v_i \in Q_2(K) \,\forall\, K \in C_h, \quad \text{for } i=1, 2\},$$

$$P_h = \{p \in L_0^2(\Omega) \mid p = p_0 + p_1, \quad p_1 \in C(\bar{\Omega}), \quad (p_1 \in Q_1(K) \quad \text{and} \quad p_0 \in Q_0(K) \,\forall\, K \in C_h\}.$$

A typical patch is illustrated in Figure 1, and without loss of generality we have taken the origin of the axes to be at the pressure node $P_3$. Over this patch a $v \in V_{0,M}$ is defined by

$$v = \frac{x(x+y)y(y-l)}{(+k^2l^2/16)}\underline{v}_1 + \frac{(x+k/2)(x+k)y(y-l)}{(-k^2l^2/8)}\underline{v}_3 \quad \text{in } K_1, \tag{6a}$$

$$v = \frac{x(x-k)y(y-l)}{(+k^2l^2/16)}\underline{v}_2 + \frac{(x-k/2)(x-k)y(y-l)}{(-k^2l^2/8)}\underline{v}_3 \quad \text{in } K_2. \tag{6b}$$

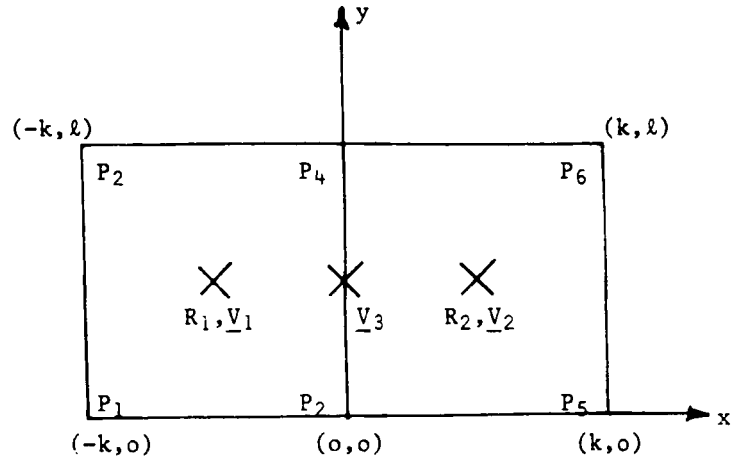


Figure 1. A macroelement of two quadrilateral elements

Similarly, a $p \in P_M$ is defined by

$$p = \frac{x(y-l)}{kl} P_1 - \frac{xy}{kl} P_2 \frac{(x+k)(y-l)}{kl} P_3 + \frac{(x+k)y}{kl} P_4 + R_1 \quad \text{in } K_1$$

$$= \tilde{p} + R_1 \quad \text{in } K_1,$$

$$p = \tilde{p} + R_2 \quad \text{in } K_2,$$

where $\tilde{p}$ is the usual $Q_1$ Taylor–Hood pressure approximation.

Following the method of proof of Stenberg, we shall successively consider particular velocities $v_t$ from $V_{0,M}$ and find the constraints on $\{P_1, P_2, \ldots, P_6, R_1, R_2\}$ such that

$$(\operatorname{div} v_t, p)_M = 0. \tag{7}$$

Initially we shall consider velocities that have zero normal components around both $\partial K_1$ and $\partial K_2$. In this case

$$(\operatorname{div} v_t, p)_M = (\operatorname{div} v_t, \tilde{p})_M$$

$$= (v_t, \nabla \tilde{p})_M \quad \because \tilde{p} \in C(\bar{M}). \tag{8}$$

We first consider $v_t$ given by (6a) and (6b) with both $\underline{v}_2 = 0$ and $\underline{v}_3 = 0$. From (7) and (8), noting that the integral of (8) is a bicubic polynomial and is integrated exactly by the product Simpson's rule, then

$$\nabla \tilde{p} = 0 \quad \text{at 1.} \tag{9}$$

Similarly, choosing $v_t$ such that $\underline{v}_1 = 0$ and $\underline{v}_2 = 0$, we obtain

$$\nabla \tilde{p} = 0 \quad \text{at 2.} \tag{10}$$

If we now take $v_t$ as the tangential velocity at node 3, i.e. $\underline{v}_1 = 0$, $\underline{v}_2 = 0$ and $(v_3)_1 = 0$, then we obtain

$$\partial \tilde{p} / \partial y = 0 \quad \text{at 3.} \tag{11}$$

The conditions (9)–(11) tell us that (7) is satisfied for every $v \in V_{0,M}$ only if $\tilde{p}$ is a constant, $P_c$ say, throughout $M$; that is, only if

$$p = P_c + R_1 \quad \text{in } K_1,$$
$$p = P_c + R_2 \quad \text{in } K_2.$$

We now choose $v_t$ equal to the normal velocity at 3. The condition (7) gives

$$0 = (\text{div } v_t, p)_M = (\text{div } v_t, P_c)_M + (\text{div } v_t, R_1)_{K_1} + (\text{div } v_t, R_2)_{K_2} = = \frac{2l}{3}(R_1 - R_2).$$

Thus $R_1 = R_2$ and $N_M$ for this patch consists of constant functions. By a similar argument, patches of two elements in the $y$-direction also have $N_M$ consisting only of constant functions. It is now possible to meet all the conditions of Theorem 2 with $q = 2$, and in order to have every interior edge in exactly one macroelement, each element will be in not more than four macroelements. Thus we conclude that the $Q_2/Q_1$ Taylor–Hood element on regular grids with the pressure space supplemented by the piecewise constants over the elements satisfies the Babuska–Brezzi compatibility condition.

*Regular grids of hexahedral elements*

In this subsection we shall assume that $C_h$ is a regular grid with grid lines parallel to the $x$-, $y$- and $z$-axes. The definitions of the velocity space $V_h$ and the pressure space $P_h$ are essentially the same as the two-dimensional case, but the velocity now has three components. A simple count of velocity nodes and pressure nodes shows that a patch or macroelement of two elements will not have a null space $N_M$ consisting only of constant functions. This case is complicated by the fact that not only do we have to consider a three-dimensional element but also we have to consider a macroelement of four elements, illustrated in Figure 2. The method of proof will be similar to that of the previous section in that we shall consider particular $v_t$ from $V_{0,M}$ and find constraints on $p \in P_M$ such that (7) is satisfied. The pressure space $P_M$ depends on the 22 parameters

$$\{P_1, P_2, \ldots, P_{18}, R_1, R_2, R_3, R_4\},$$

where $P_i$ is the pressure at the $i$th vertex (see Figure 2) and $R_1$ is the constant pressure in the $i$th element $K_i$. We note that $\{P_1, \ldots, P_{18}\}$ is the 'Taylor–Hood' pressure and we can write a typical $p \in P_M$ as

$$p = \tilde{p} + R_i \quad \text{in } K_i,$$

where $\tilde{p}$ is the continuous, piecewise bilinear Taylor–Hood pressure. Again we begin by considering $v_t$ that have zero normal components around the edges of all four elements in the macroelement such that equation (8) is satisfied.

We first choose $v_t$ such that its only non-zero nodal parameter is the $y$-component at the midpoint of the line (5, 4) from node 5 to 4. After a certain amount of manipulation,

$$(\text{div } v_t, p)_M = \frac{4km}{27}(P_5 - P_{14}) = 0, \tag{12}$$

from which we conclude that

$$P_5 = P_{14} \equiv P_c. \tag{13}$$

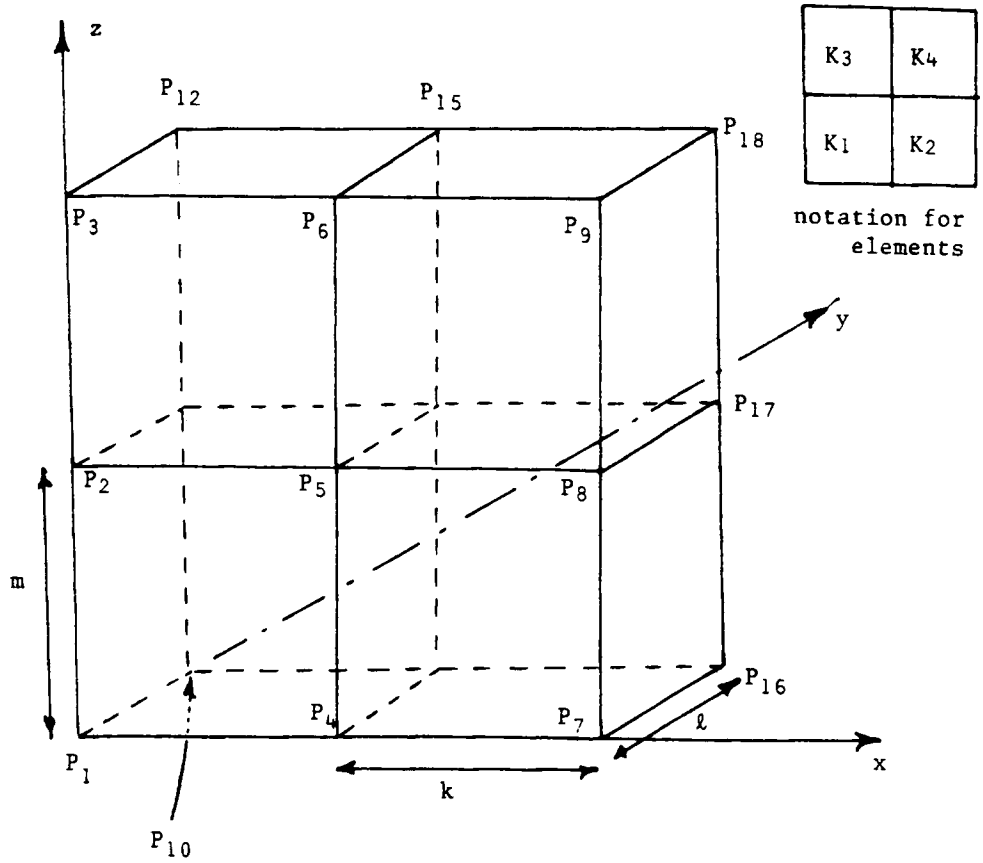


Figure 2. A macroelement of four hexahedral elements

We now choose $v_t$ such that its only non-zero nodal parameter is the $y$-component at the midpoint of the face (4, 13, 14, 5); then

$$(\text{div } v_t, p)_M = \frac{2km}{27}(P_4 + P_5 - P_{13} - P_{14}) = 0. \tag{14}$$

Similarly, taking $v_t$ such that its only non zero-nodal parameter is the $z$-component at the midpoint of the face (4, 13, 14, 5), then

$$(\text{div } v_t, p) = \frac{2kl}{27}(P_4 + P_{13} - P_5 - P_{14}) = 0. \tag{15}$$

From equations (13)–(15) we conclude that

$$P_{13} = P_4 = P_c.$$

We now consider each of the other three inner faces in turn and let $v_t$ be velocities tangential to these planes. We conclude that if $p \in P_M$ and (7) is satisfied for every $v \in V_{0,M}$, then

$$P_2 = P_4 = P_5 = P_6 = P_8 = P_{11} = P_{13} = P_{14} = P_{15} = P_{17} = P_c. \tag{16}$$

To continue, we choose $v_t$ such that its only non-zero nodal component is the $x$-component at the centroid of (1, 4, 13, 10, 2, 5, 14, 11), i.e. element $K_1$. Thus

$$(\text{div } v_t, p)_M = \frac{2lm}{27}(P_1 + P_2 + P_{10} + P_{11} - P_4 - P_5 - P_{12} - P_{13}) = 0. \tag{17}$$

Choosing $v_t$ such that its only non-zero nodal component is the $y$-component at the centroid of $K_1$, we obtain

$$(\text{div } v_t, p)_M = \frac{2km}{27}(P_1 + P_2 + P_4 + P_5 - P_{10} - P_{11} - P_{13} - P_{14}) = 0. \tag{18}$$

Equations (16)–(18) give us

$$P_1 = P_{10} = P_c.$$

Progressing through the elements, we obtain the result that

$$P_i = P_c \quad \text{for } i = 1, 2, \ldots, 18,$$
$$p = P_c + R_i \quad \text{in} \quad K_i \quad \text{for } i = 1, 2, 3, 4. \tag{19}$$

Finally we choose $v_t$ such that its only non-zero nodal parameter is the normal component at the centroid of the plane (4, 13, 14, 5) (i.e. the $x$-component), and using (19) we obtain

$$\frac{16\,lm}{9}(R_1 - R_2) = 0, \quad \text{i.e. } R_1 = R_2.$$

Choosing $v_t$ such that its only non-zero nodal parameter is the normal component at the centroid of the other inner faces, we conclude that

$$R_1 = R_2 = R_3 = R_4. \tag{20}$$

Thus (19) and (20) give us the required result that $N_M$ for this macroelement consists of constant functions only.

If we consider this macroelement as a '$(2 \times 1 \times 2)$' macroelement, then a similar argument will apply for '$(2 \times 2 \times 1)$' and '$(1 \times 2 \times 2)$' macroelements. Thus any grid made up of these three macroelements will satisfy Theorem 2 and hence the Babuska–Brezzi compatibility result. We note that in the course of this proof we have also established that the $Q_2/Q_1$ Taylor–Hood hexahedral element on regular grids also satisfies (3).

*Irregular grids of $Q_2/Q_1$ elements*

Spurious pressure modes invariably show up on regular grids and often are not present on irregular grids, but for completeness the Babuska–Brezzi condition (3) should be established for all grids.

In two dimensions the Taylor–Hood element on irregular grids is shown to satisfy (3) by Stenberg.[7] This proof, with minor modifications, establishes that $N_M$ for two-element macroelements consists of constant pressures. The modification required to Stenberg's proof is that care is required on the inner side. Stenberg arbitrarily chose $v_t$ such that its only non-zero nodal parameter was one of the components at the centre of the side. For the augmented Taylor–Hood element it is necessary to first choose $v_t$ such that it is along the side and then choose $v_t$ such that it is normal to the side.

In three dimensions the situation is much more complicated. The argument in the above subsection does not seem to generalise in a simple way. The main reason for this is that the edges of

a general quadrilateral are straight lines but the faces of a general hexahedron are *not* flat planes. In all tests carried out, blocks of four distorted $Q_2/Q_1$ elements have an $N_M$ that consists of constant functions, but this does not establish the required result. It seems then that it is still an open question whether the $Q_2/Q_1$ Taylor–Hood or augmented Taylor–Hood element on irregular grids in $R^3$ satisfies the condition (3).

*The $P_2/P_1$ triangular element*

The $P_2/P_1$ triangular element remains a popular element for two-dimensional flow. The pressure space for this element can be augmented by piecewise constants to produce an element that is mass-conserving over each element of the grid. The velocity and pressure spaces are

$$V_h = \{u \in (H^1(\Omega))^2 \mid v_i \in P_2(K) \,\forall\, K \in C_h,\ i = 1, 2\},$$

$$P_h = \{p \in L_0^2(\Omega) \mid p = p_0 + p_1,\ p_1 \in C(\Omega),\ p_1 \in P_1(K) \quad \text{and} \quad p_0 \in P_0(K) \,\forall\, K \in C_h\}.$$

To prove that this element satisfies (3), we shall first consider the two-element patch $\tilde{M}$ illustrated in Figure 3. We choose $v_t \in V_{0,\tilde{M}}$ and find the constraints on $p$ such that $(\text{div } v_t, p)_{\tilde{M}} = 0$. The space $P_{\tilde{M}}$ is defined by

$$p = P_1 L_1 + P_2 L_2 + P_4 L_3 + R_1 \quad \text{in } K_1,$$

$$p = P_3 L_1 + P_4 L_2 + P_2 L_3 + R_2 \quad \text{in } K_2.$$

The space $V_{0,\tilde{M}}$ is only two-dimensional as determined by the two components at the midside of the inner side of $\tilde{M}$. Choosing $v_t$ parallel to this side, we obtain

$$(\text{div } v_t, p)_{\tilde{M}} = \frac{h_1 + h_2}{6}(P_2 - P_4) = 0, \quad \text{i.e. } P_2 = P_4 \equiv P_c. \tag{21}$$

Choosing $v_t$ normal to the inner side and using (21), we obtain

$$(\text{div } v_t, p)_{\tilde{M}} = +l[P_3 - P_1 + 4(R_2 - R_1)]/6. \tag{22}$$

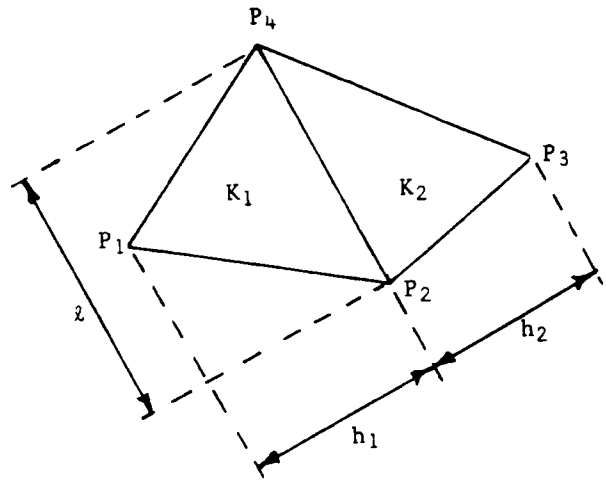


Figure 3. The two-element patch $\tilde{M}$ of triangles

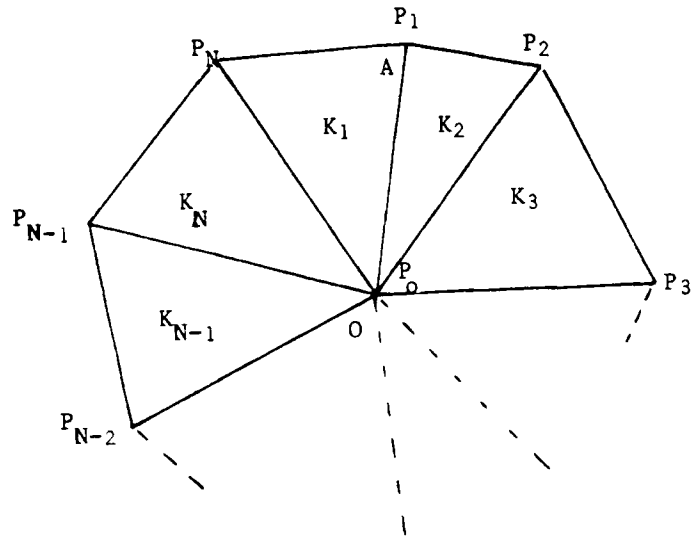


Figure 4. A macroelement of triangular elements

The two-element patch illustrated in Figure 3 is not a suitable macroelement, but that illustrated in Figure 4 is. In Figure 4 we have $N$ elements each with two sides in common with other elements of the patch, and they all share a common internal node. By considering $v_t$ parallel to the side (0, A), with the only non-zero nodal parameter at the midpoint of that side, we obtain, using (21),

$$P_0 = P_1 \equiv P_c.$$

Repeating this argument for each of the $N$ sides, then

$$P_0 = P_1 = P_2 = \ldots = P_N \equiv P_c. \tag{23}$$

Now taking $v_t$ normal to the side (0, A), with the only non-zero parameters at the midpoint of that side, we obtain, using (22) and (23),

$$R_1 = R_2.$$

Repeating this argument for each of the $N$ sides, we find that $N_M$ for this macroelement illustrated in Figure 4 consists of constant functions. Thus grids that are made up of a fixed number of classes of such macroelements will satisfy (3). This does of course mean that on any grid we must 'triangulate into the corners'.

## 3. NUMERICAL EXAMPLES

In this section we shall consider two numerical examples. The first is a simple test problem to demonstrate that optimal convergence rates are achieved and the second is an example where the $P_2/P_1$ Taylor–Hood element gives poor results but the augmented element gives relatively good results.

*Testing rates of convergence*

The first test problem is one proposed by Griffiths.[12] It is an enclosed flow problem (namely a Stokes flow) in the unit square with solution

$$\begin{aligned} V_x &= -20xy^3, \\ V_y &= 5y^4 - 5x^4, \\ p &= -60x^2y + 20y^3 + 5. \end{aligned} \tag{24}$$

Typical grids for this test problem are illustrated in Figure 5. The solutions (i.e. norms of errors) are presented in Table I, with the results compared for the Taylor–Hood element, its augmented version and the bubble element (quadratic plus bubble velocities, fully discontinuous pressures).[9] It can be seen that the errors for the two versions of the Taylor–Hood element are comparable and both much smaller than the Girault–Raviart bubble element for this problem. Moreover, for all three elements the optimal convergence rates are observed.

*Illustrating difficulties with the Taylor–Hood element*

The solution of a non-Newtonian fluid in the volume of revolution of the region illustrated in Figure 6, with the $V_\theta$ boundary conditions given in the figure, can be reduced to solving the set of equations

$$\frac{1}{Re}\left(\frac{\partial^2 V_r}{\partial r^2} + \frac{\partial^2 V_r}{\partial z^2} + \frac{1}{r}\frac{\partial V_r}{\partial r} - \frac{V_r}{r^2}\right) - \frac{\partial p}{\partial r} = -\frac{N_n V_\theta^2}{r} + N_\theta\left[\left(\frac{\partial V_\theta}{\partial r} - \frac{V_\theta}{r}\right)^2 + \left(\frac{\partial V_\theta}{\partial r}\right)\right], \tag{25a}$$

$$\frac{1}{Re}\left(\frac{\partial^2 V_\theta}{\partial r^2} + \frac{\partial^2 V_\theta}{\partial z^2} + \frac{1}{r}\frac{\partial V_\theta}{\partial r} - \frac{V_\theta}{r^2}\right) = 0, \tag{25b}$$

$$\frac{1}{Re}\left(\frac{\partial^2 V_z}{\partial r^2} + \frac{\partial^2 V_z}{\partial z^2} + \frac{1}{r}\frac{\partial V_z}{\partial r}\right) - \frac{\partial p}{\partial z} = 0, \tag{25c}$$

$$\frac{\partial V_r}{\partial r} + \frac{V_r}{r} + \frac{\partial V_z}{\partial z} = 0 \tag{25d}$$

after a number of assumptions have been made, further details of which are given by Tidd.[13] The $V_r$ and $V_z$ boundary conditions are homogeneous Dirichlet conditions. For a Newtonian fluid the

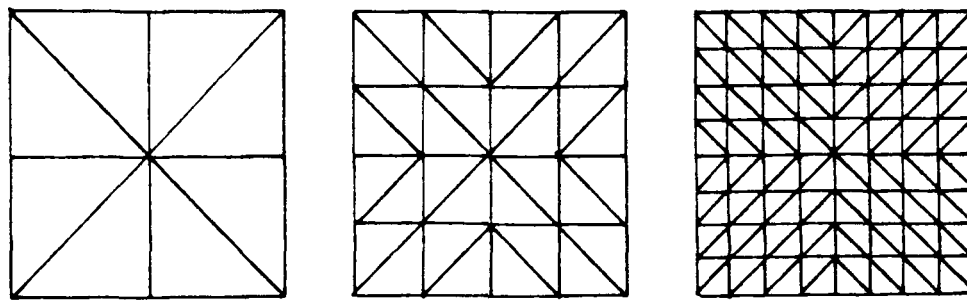


Figure 5. Grids for the first test problem

Table I. Results for test problem 1

| | Errors | | |
|---|---|---|---|
| | $\|p\|_{L_0^2(\Omega)}$ | $\|\underline{V}\|_{H^1(\Omega)}$ | $\|\underline{V}\|_{L^2(\Omega)}$ |
| 4 × 4 | 0·4283 | 0·4802 | 0·01669 |
| 8 × 8 | 0·0975 | 0·1189 | 0·00239 |
| 16 × 16 | 0·0233 | 0·0296 | 0·00029 |
| Order | ~2 | ~2 | ~3 |
| Element | Taylor–Hood | | |
| 4 × 4 | 0·4878 | 0·4865 | 0·01637 |
| 8 × 8 | 0·1009 | 0·1190 | 0·00237 |
| 16 × 16 | 0·0233 | 0·0296 | 0·00029 |
| Element | Augmented Taylor–Hood | | |
| 4 × 4 | 1·5469 | 0·6834 | 0·02416 |
| 8 × 8 | 0·4314 | 0·1797 | 0·00342 |
| 16 × 16 | 0·1142 | 0·0462 | 0·00043 |
| Order | ~2 | ~2 | ~3 |
| Element | Quadratic + bubble velocity/discontinuous linear pressure | | |

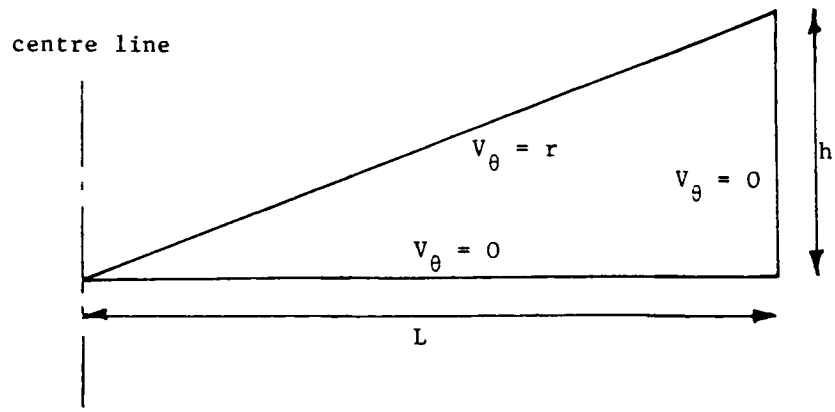


Figure 6. The second test problem ($L = 1{\cdot}0$, $h = 0{\cdot}1$)

parameter $N_e = 0$ and for a non-Newtonian fluid this parameter gives a measure of the non-Newtonian effects. We note that equation (25b) is independent of $V_r$, $V_z$, $p$ and $N_e$ and decouples from the other three equations, whereas equations (25a), (25c) and (25d) represent a Stokes flow problem in $(r, z)$ co-ordinates. This can be solved for the two cases ($N_n = 1$, $N_e = 0$) and ($N_n = 0$, $N_e = 1$) and the particular solution required can be obtained by selecting the required ratio of these two intermediate solutions.

The main flow in this problem is a $V_\theta$ flow with $V_r$ and $V_z$ representing secondary flows. Indications of the secondary flows for the three cases ($N_n = 1$, $N_e = 0$), ($N_n = 0$, $N_e = 1$) and ($N_n = 1$,

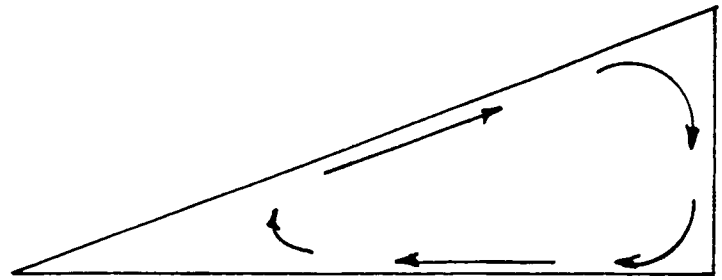

$N_n = 1, \quad N_e = 0$

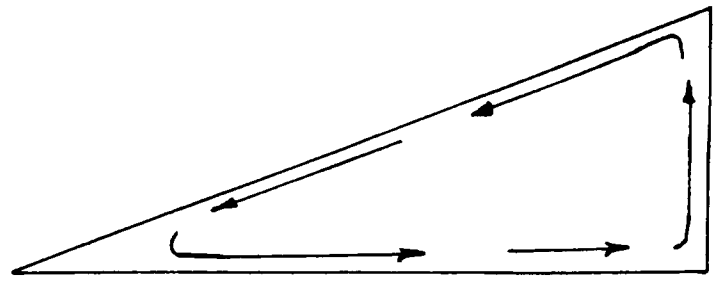

$N_n = 0, \quad N_e = 1$

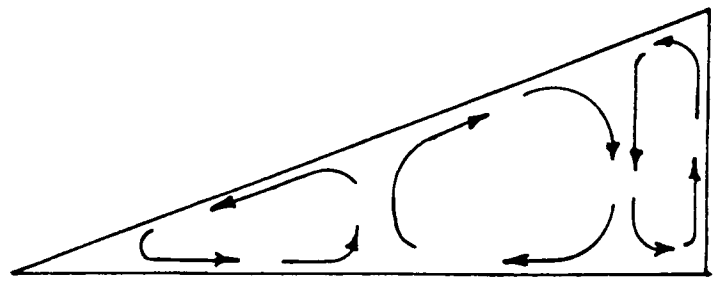

$N_n = 1, \quad N_e = 1/9$

Figure 7. Illustrating secondary recirculations ($Re = 10$)

$N_e = 1/9$) are given in Figure 7. The three secondary recirculations of the third case have been observed by Hoppmann and Baronet,[14] and it is in attempting to model these three recirculations that we find that the Taylor–Hood element gives a very poor solution even on a highly refined grid. A typical grid used is illustrated in Figure 8. The $V_\theta$ problem, namely equation (25b), was solved on each of the grids. On a given grid the relevant $V_\theta$ numerical solution was used on the right-hand side of equation (25a).

We find that the Taylor–Hood and its augmented version give essentially the same results for the case ($N_n = 1$, $N_e = 0$) but very different answers for the case ($N_n = 0$, $N_e = 1$), with the augmented version giving far more consistency from one grid to the next. Moreover, for the case ($N_n = 1$, $N_e = 1/9$), where we are expecting to observe three recirculations, the Taylor–Hood element gives only one complete recirculation with velocities in almost random directions over essentially half the region of the problem, namely $0 \leq r \leq 0{\cdot}5$, even on the highly refined $64 \times 16$

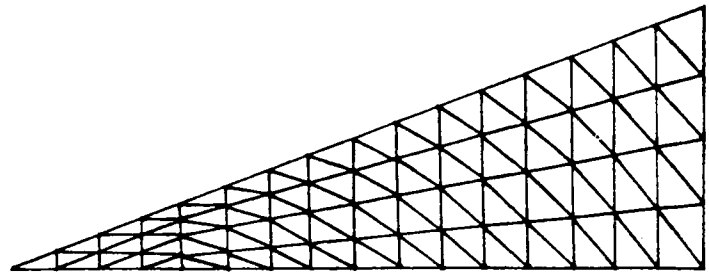

Figure 8. A typical grid (16 × 4) for the second test problem

grid. However, the augmented version resolves all three recirculations on a 16 × 4 grid and gives very good consistency between the 32 × 8 and 64 × 16 grids. The bubble element performed in a similar manner to the augmented Taylor–Hood element, giving somewhat less accurate answers for a greater cost.[15] We also note that the problem does not fall into the analysis given above. Not only is the problem in $(r, z)$ co-ordinates but also we have not triangulated into all the corners. By modifying the grid so that we do triangulate into all the corners, the solutions obtained do not change in any significant way.

## 4. FINAL REMARKS

In this paper we have analysed and given some examples of the use of supplementing the pressure space of Taylor–Hood elements by piecewise constants. This process has the advantage of making the element locally mass-conserving. Two examples are given: one illustrates that the expected rate of convergence is achieved in practice and the second illustrates a much improved performance over the standard Taylor–Hood element. Both these examples illustrate that for these problems the augmented Taylor–Hood element outperforms the use of bubble functions.

## REFERENCES


1. P. Hood and C. Taylor, 'Navier–Stokes equations using mixed interpolation', in *Finite Element Methods in Flow Problems*, UAH Press, Huntsville, AL, 1974, pp. 121–132.
2. P. M. Gresho, R. L. Lee, S. T. Chan and J. M. Leone, 'A new finite element for Boussinesq fluids', in *Proc. Third Int. Conf. on Finite Elements in Flow Problems*, Wiley, 1980, pp. 204–215.
3. B. Debbaut and M. Crochet, 'Further results on the flow through on abrupt contraction', *J. Non-Newtonian Fluid Mech.*, **20**, 173–185 (1986).
4. D. M. Tidd, R. W. Thatcher and A. Kaye, 'The free surface flow of Newtonian and non-Newtonian fluids trapped by surface tension', *Int. j. numer. method fluids*, **8**, 1011–1027 (1988).
5. D. F. Griffiths, 'The effect of pressure approximation on finite element calculations of incompressible flows', in K. W. Morton and M. J. Baines (eds). *Numerical Methods for Fluid Dynamics*, Academic Press, pp. 359–374, 1982.
6. J. M. Boland and R. A. Nicolaides, 'Stability of finite elements under divergence constraints', *SIAM J. Numer. Anal.*, **20**, 722–731 (1983).
7. R. Stenberg, 'Error analysis of some finite element methods for the Stokes problem', *Math. Comput.*, **42**, 9–32 (1989).
8. R. Verfurth, 'Error estimates for a mixed finite element approximation of the Stokes equations', *RAIRO Anal. Numer.*, **18**, 175–182 (1984).
9. V. Girault and P. A. Raviart, '*Finite Element Methods for Navier–Stokes Equations*, Springer, New York, 1986.
10. R. Stenberg, 'Analysis of mixed finite element methods', *Math. Comput.*, **42**, 9–23 (1984).
11. P. Ciarlet, *The Finite Element Method Elliptic Problems*, North-Holland, Amsterdam, 1977.
12. D. F. Griffiths, 'Finite elements for incompressible flows', *Math. Methods Appl. Sci.*, **1**, 16–31 (1979).
13. D. M. Tidd, 'Finite element calculations for flow in reogoniometers with a free surface', *Ph.D. Thesis*, UMIST, Manchester, 1987.
14. W. H. Hoppman and C. N. Baronet, 'Study of flow induced in a viscoelastic liquid by a rotating core', *Trans. Soc. Rheol.*, **9**, 417–423 (1965).
15. A. Henly, 'A comparison of finite element solutions for solving a fluid flow problem with rotational symmetry, *M.Sc. Dissertation*, University of Manchester, 1988.